

# Polarized reflectance measurements of the CDW transitions in $\eta$ -Mo<sub>4</sub>O<sub>11</sub> and $\gamma$ -Mo<sub>4</sub>O<sub>11</sub>

A. W. McConnell and B. P. Clayman

*Department of Physics, Simon Fraser University, Burnaby, British Columbia, V5A 1S6, Canada*

C. C. Homes

*Department of Physics, Brookhaven National Laboratory, Upton, New York 11973-5000*

M. Inoue and H. Negishi

*Graduate School of Advance Sciences of Matter, Semiconductor Physics Laboratory,  
Kagamiyama 1-3-1, Higashi-Hiroshima 739-8526, Japan*

(Received 8 January 1998; revised manuscript received 29 June 1998)

Temperature-dependent (300–10 K) reflectance measurements were made on  $\eta$ -Mo<sub>4</sub>O<sub>11</sub> and  $\gamma$ -Mo<sub>4</sub>O<sub>11</sub> in the conducting  $b$ - $c$  plane in the frequency range 30–8000 cm<sup>-1</sup>, for light polarized both parallel and perpendicular to the charge density wave (CDW) direction ( $b$  axis). The optical conductivity was determined from a Kramers-Kronig analysis of the reflectance. The data clearly show strong suppression of the conductivity in the  $c$ -axis direction below the CDW transition temperatures, leading to a partial optical gap in the spectrum. The  $b$ -axis conductivity does not show as strong a suppression except at low frequencies. The CDW gap energies for both crystals are evaluated, in agreement with those obtained from transport data. The data are considered in light of recent work on stripes and charge ordering in the field of superconductivity.

[S0163-1829(98)05644-6]

## I. INTRODUCTION

It has been known since 1983 that the two phases of Mo<sub>4</sub>O<sub>11</sub> exhibit incommensurate charge-density wave (CDW) transitions.<sup>1</sup> The monoclinic phase  $\eta$ -Mo<sub>4</sub>O<sub>11</sub> has a transition at  $T_{C1}$  = 105 K with a CDW wave vector  $\mathbf{q}_{CDW}$  = 0.23 $b^*$  and another at  $T_{C2}$  = 35 K with the in-plane nesting vector (0.42 $b^*$ , 0.28 $c^*$ ) (Ref. 2). The orthorhombic phase  $\gamma$ -Mo<sub>4</sub>O<sub>11</sub> has a single transition at  $T_C$  = 100 K with  $\mathbf{q}_{CDW}$  = 0.23 $b^*$ . Extensive transport measurements have been performed on these two phases including resistivity,<sup>1,3-5</sup> transverse magnetoresistance,<sup>4,6</sup> and Hall effect.<sup>5,6</sup> The conduction electrons are known<sup>7</sup> to be confined in the  $b$ - $c$  plane, resulting in quasi-two-dimensional electronic properties. The CDW transitions are metal-metal transitions, with the crystals remaining metallic down to the lowest temperatures measured. From transport measurements, the CDW gap energies at  $T_{C1}$  and  $T_{C2}$  for  $\eta$ -Mo<sub>4</sub>O<sub>11</sub> are determined:  $2\Delta_1 \approx 32$  meV (260 cm<sup>-1</sup>) and  $2\Delta_2 \approx 9.0$ –9.7 meV (73–78 cm<sup>-1</sup>), respectively,<sup>4,5,8</sup> while the value for  $\gamma$ -Mo<sub>4</sub>O<sub>11</sub> is  $2\Delta \approx 13$  meV (105 cm<sup>-1</sup>) (Refs. 5 and 9). This last is much smaller than the maximum gap opening determined from recent angle-resolved photoemission measurements  $2\Delta_{MAX} = 60 \pm 10$  meV ( $\approx 480$  cm<sup>-1</sup>).<sup>10</sup>

Some optical measurements have been performed on the Mo<sub>4</sub>O<sub>11</sub> phases, although surprisingly few considering the extensive use made of optical and related techniques in investigating other one-dimensional (1D) CDW materials such as K<sub>0.3</sub>MoO<sub>3</sub> (Refs. 11 and 12). This could perhaps be due to the difficulty in accurately measuring the very small temperature-dependent changes in the reflectance spectra. The far-infrared (FIR) region was measured by Guyot *et al.*<sup>13</sup> for incident radiation polarized along the  $a$  axis for mosaics of single crystals of both phases. This work clearly estab-

lished that the  $a$  axis is semiconducting, although no measurements were made below 300 cm<sup>-1</sup> and no results for the conducting  $b$ - $c$  plane were shown. The resulting spectra showed very strong phonons that were fit using the factorized model of the dielectric function. The reflectance was not compared to a well-known standard such as Al or Au; instead the overall level of reflectance was adjusted assuming that a measurement of the reflectance along the  $b$  axis was  $\approx 100\%$ . This would lead to incorrect levels although the phonon structure should remain the same. A single frequency measurement at 1100 cm<sup>-1</sup> showed a difference in reflectance of almost 60% between the  $b$  and  $c$  axes at room temperature.

Some unpolarized diffuse-reflectance spectra of powder samples have also been reported.<sup>14</sup> In this study, a variety of elements (W,V,Re) are partially doped into the Mo sites. The changes in the spectrum both as functions of doping and temperature are shown from about 200 cm<sup>-1</sup> to 50 000 cm<sup>-1</sup> but no attempt was made to establish absolute levels of reflectance. A metal-insulator transition is seen as the doping level is increased. Some reflectance measurements were done in the visible on  $\gamma$ -Mo<sub>4</sub>O<sub>11</sub> to investigate the anisotropy of the color properties, which are seen in both phases.<sup>15,16</sup> The authors describe the color anisotropy of these materials—purple along the  $c$  axis, blue along the  $b$  axis, and gold along the  $a$  axis—and discuss this effect within the context of a simple band model. Very recent work has been done by Zhu *et al.*<sup>17</sup> in measuring the temperature dependence of the reflectance at infrared and higher frequencies, 5000 to  $\approx 35$  000 cm<sup>-1</sup>. The reflectance and its functional form agree well with ours within the region of overlap.

Optical reflectance work on similar quasi-two-dimensional molybdenum bronzes, the “purple bronzes,” A<sub>0.9</sub>Mo<sub>6</sub>O<sub>17</sub> ( $A = \text{K or Na}$ ) has been reported by Degiorgi

*et al.*<sup>18</sup> Although no plots of optical conductivity  $\sigma_1(\omega)$  are given, the reflectance remains high ( $>80\%$ ) below  $1000\text{ cm}^{-1}$ . A small dip in reflectance is observed at temperatures below the proposed measured optical gap edge and there is an accompanying increase in reflectance above the gap edge. No phonon structure was seen in these materials at any of the temperatures measured and no significant anisotropy in the conducting plane reflectance was observed. The increased reflectance above the dip was proposed to be due to a peak at the optical gap edge as is seen in 1D systems.

The purpose of this study was to compare the optical features of a two-dimensional (2D) CDW system to features predicted and seen in 1D systems. To this end, we have measured the temperature-dependent reflectance of both phases of  $\text{Mo}_4\text{O}_{11}$ , polarized parallel ( $b$  axis) and perpendicular ( $c$  axis) to the CDW, in the far-infrared and the near-infrared regions ( $30$  to  $\approx 8000\text{ cm}^{-1}$ ). The reflectance spectra were taken for a variety of temperatures above and below the CDW transitions.

## II. EXPERIMENT

The experiments were performed using a Bruker IFS 113V Fourier-transform spectrometer with various combinations of sources and detectors. In the FIR region ( $30$ – $1000\text{ cm}^{-1}$ ) a Hg arc lamp was the source and a Si  $4.2\text{ K}$  bolometer was the detector; the resolution was  $2\text{ cm}^{-1}$ . In the mid-infrared (MIR) region, a globar was used with a liquid-nitrogen-cooled MCT semiconductor detector with resolution varying from  $8\text{ cm}^{-1}$  at low frequencies ( $1000$ – $4000\text{ cm}^{-1}$ ) to  $20\text{ cm}^{-1}$  at higher frequencies ( $3500$ – $8000\text{ cm}^{-1}$ ). Samples were mounted on a He flow cryofinger, which allowed cooling of the samples to  $10\text{ K}$ . An *in situ* gold deposition technique<sup>19</sup> allowed accurate determination of the absolute reflectance of the samples. The typical uncertainty in absolute reflectance in the FIR region is only  $\pm 0.5\%$ . This level of accuracy is necessary due to the very small changes that occur in the reflectance spectra as a function of temperature, particularly at temperatures around the transitions.

The  $\text{Mo}_4\text{O}_{11}$  crystals were grown by chemical vapor transport at Hiroshima University; the growth details are given elsewhere.<sup>4,8</sup> The samples were optically flat single crystals  $\sim 4 \times 4 \times 0.1\text{ mm}^3$  with the thin dimension along the  $a$  axis. This allowed easy measurements of the  $b$ - $c$  plane. No polishing or other surface preparation was used.

The optical properties are calculated from a Kramers-Kronig analysis of the reflectance. For all temperatures, a metallic Hagen-Rubens ( $1 - R \propto \sqrt{\omega}$ ) extrapolation was used at low frequencies. For the high-frequency extrapolation, spectra measured by Zhu *et al.*<sup>17</sup> were used out to  $\approx 35\,000\text{ cm}^{-1}$ , above which a free-electron behavior ( $R \propto \omega^{-4}$ ) was assumed.

## III. RESULTS

The  $b$ - and  $c$ -axis FIR reflectance spectra for  $\eta$ - $\text{Mo}_4\text{O}_{11}$  and  $\gamma$ - $\text{Mo}_4\text{O}_{11}$  are shown in Figs. 1 and 2, respectively. The reflectance spectra of both materials are “metalliclike” even down to  $10\text{ K}$  throughout most of the spectral range. As the temperature is lowered through the first CDW transition, the reflectance spectra change at most by  $4\%$ , in contrast to the

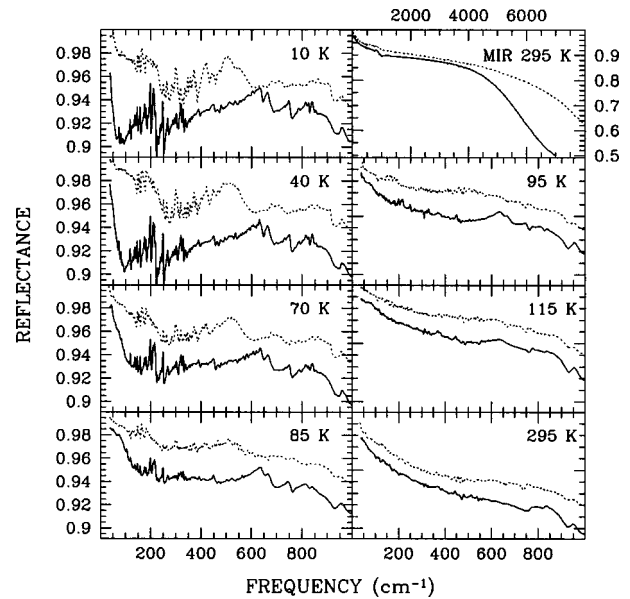


FIG. 1. Reflectance of  $\eta$ - $\text{Mo}_4\text{O}_{11}$  for a variety of temperatures, as labeled in the upper-right corner. Both the  $b$  axis (dotted curve) and the  $c$  axis (solid curve) are shown for each temperature. The spectra labeled MIR are the  $295\text{ K}$  spectra for the full range measured.

large reductions seen in the reflectance levels of 1D materials such  $\text{K}_{0.3}\text{MoO}_3$  (Refs. 11 and 12) of up to  $40\%$  or more in this spectral range. This small change in the spectra as a function of temperature underlines the necessity for accuracy in the absolute reflectance levels.

We see a suppression of reflectance in the frequency range  $50$  to  $\approx 400\text{ cm}^{-1}$  in  $\eta$ - $\text{Mo}_4\text{O}_{11}$  and  $\gamma$ - $\text{Mo}_4\text{O}_{11}$  and there is an increase in reflectance in the frequency range between  $400$  and  $1000\text{ cm}^{-1}$ . This is similar to what was

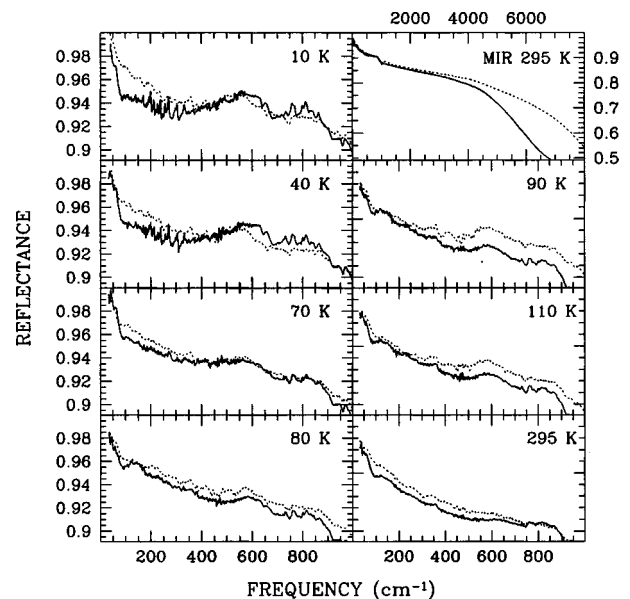


FIG. 2. Reflectance of  $\gamma$ - $\text{Mo}_4\text{O}_{11}$  at a variety of temperatures labeled in the upper-right corner of each plot. Both the  $b$  axis (dotted curve) and the  $c$  axis (solid curve) are shown for each temperature. The spectra labeled MIR are the  $295\text{ K}$  spectra for the full range measured.

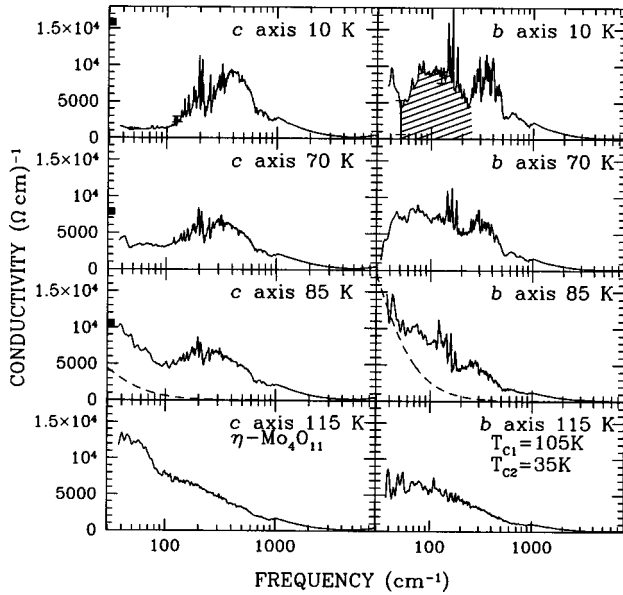


FIG. 3. Optical conductivity of  $\eta$ - $\text{Mo}_4\text{O}_{11}$  for four temperatures, as labeled in the upper-right corner. The spectra for light polarized along both the  $b$  axis and the  $c$  axis are shown for each temperature. The crosshatched region on the  $b$ -axis 10 K curve indicates the excess spectral weight seen in this polarization. The black squares seen in some plots mark the published (Ref. 3) dc conductivity from transport measurements. If no black square is seen then the conductivity is larger than the conductivity range shown. In the 10 K plots are error bars at 50 and 125  $\text{cm}^{-1}$  showing typical uncertainties for a variation of 0.5% in reflectance level.

seen in the “purple bronzes” and was likely associated with the peak at the edge of the optical gap. At 1100  $\text{cm}^{-1}$  and room temperature, the difference in reflectance between the  $b$  and the  $c$  axes for  $\eta$ - $\text{Mo}_4\text{O}_{11}$  or  $\gamma$ - $\text{Mo}_4\text{O}_{11}$  is only at most 2.5%, in contrast to the 60% measured by Guyot *et al.*<sup>13</sup> Scaling our data to assume that the  $b$  axis is 100% will only increase this difference to at most 3%. The reason for this discrepancy is unclear.

The calculated optical conductivity is shown in Figs. 3 and 4 for  $\eta$ - $\text{Mo}_4\text{O}_{11}$  and  $\gamma$ - $\text{Mo}_4\text{O}_{11}$ , respectively. Note that the error bars in the 10 K plots are the uncertainty in the optical conductivity assuming changes of  $\pm 0.5\%$  in the original reflectance spectra. In the normal state, above the CDW transition, the conductivity has an essentially metallic form. At temperatures just above the first CDW transitions (110 and 115 K in  $\gamma$ - $\text{Mo}_4\text{O}_{11}$  and  $\eta$ - $\text{Mo}_4\text{O}_{11}$ , respectively) the conductivity in both polarizations is similar, lending support to the observation that these materials can be treated as 2D metals. However, differences become more apparent as the samples are cooled below their respective transition temperatures.

We should note that the reduction in the  $\eta$ - $\text{Mo}_4\text{O}_{11}$  optical conductivity at low frequencies can be seen clearly as the temperature is lowered well below  $T_{C2}$ . The 10 K  $c$ -axis conductivity shows the reduction most clearly, while in the  $b$ -axis spectrum at 10 K there is still some residual spectral weight remaining in the 50–250  $\text{cm}^{-1}$  region (seen in Fig. 3 as the cross-hatched region).

In both polarizations,  $\eta$ - $\text{Mo}_4\text{O}_{11}$  displays an increase of conductivity in the 300–500  $\text{cm}^{-1}$  region as temperature is lowered. This takes the form of a very broad peak centered at

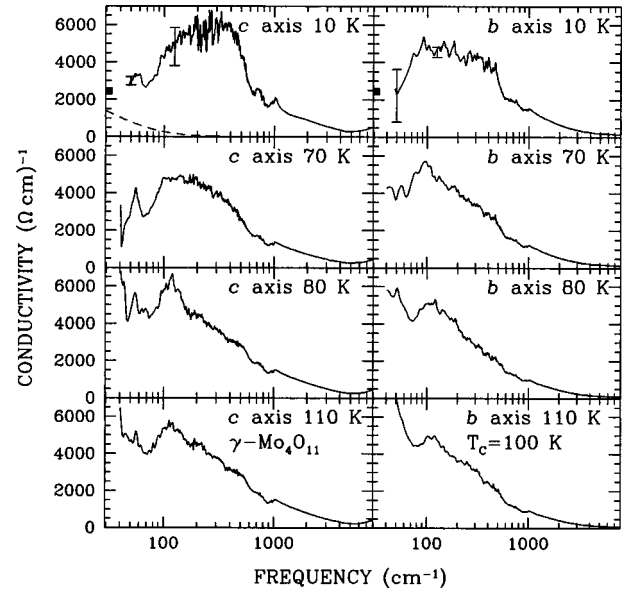


FIG. 4. Optical conductivity of  $\gamma$ - $\text{Mo}_4\text{O}_{11}$  for four temperatures, as labeled in the upper-right corner. The spectra for light polarized along the  $b$  axis and the  $c$  axis are shown for each temperature. The black squares seen in some plots mark the published (Ref. 3) dc conductivity from transport measurements. If no black square is seen then the conductivity is larger than the conductivity range shown. In the 10 K plots are error bars at 50 and 125  $\text{cm}^{-1}$  showing typical uncertainties for a variation of 0.5% in reflectance level.

$\approx 400 \text{ cm}^{-1}$ . In Fig. 4, the suppression of the  $\gamma$ - $\text{Mo}_4\text{O}_{11}$  conductivity is only visible at 10 K and below  $\approx 100 \text{ cm}^{-1}$ ; in both polarizations there is a similar increase in conductivity above this suppression but to a lesser degree than is seen in  $\eta$ - $\text{Mo}_4\text{O}_{11}$ .

No phonons are seen in the spectra above the CDW transitions,  $T_{C1}$  ( $T_C$ ). When the free carriers start to form a CDW, peaks corresponding to optically active phonons become visible in the spectrum between 100–600  $\text{cm}^{-1}$ . Unfortunately, this limits the potential detection of shifts in phonon energies related to the CDW transition to temperatures below the transition. As the temperature is lowered below  $T_{C1}$ , the peaks increase in height and decrease in width. However, no significant changes in position of the peaks is noted as a function of temperature. The sudden appearance of the phonons at the transition temperature is unusual since the conductivity does not change significantly in this frequency range and suggests that the peaks are not simply the normal infrared active modes becoming visible. Assuming that the phonons are screened by free carriers above the transition temperature, the Thomas-Fermi screening length  $l_{TF}$  can be calculated,

$$l_{TF} = 1/\sqrt{4(3/\pi)^{1/3}n_0^{1/3}/a_0} \quad (1)$$

and only changes from 0.65–0.7 Å at 115 K to 0.92–1.06 Å at 85 K. This change of screening hardly seems large enough to suggest that the infrared active phonons are becoming visible as the screening is reduced.

Figure 5 shows the frequency range of the phonons expanded for the 10 K  $\eta$ - $\text{Mo}_4\text{O}_{11}$   $b$ - and  $c$ -axes spectra. The line shapes of the phonons are seen to change as a function of frequency with the phonons becoming broader and more

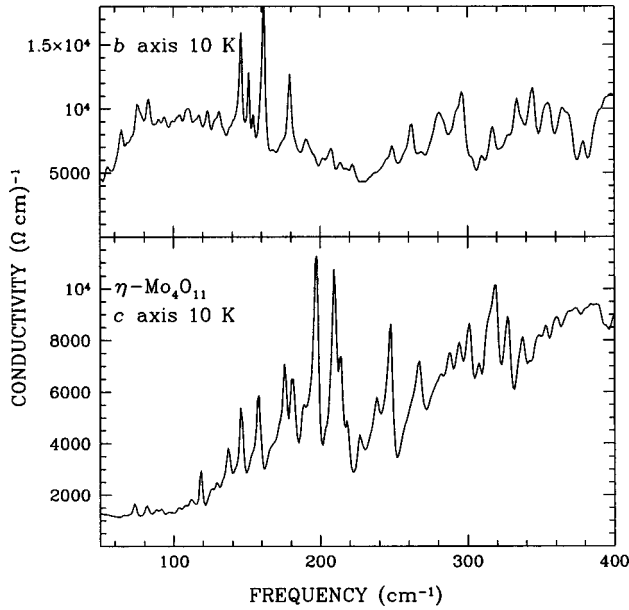


FIG. 5. Expanded view of the phonons seen in  $\eta$ - $\text{Mo}_4\text{O}_{11}$  at 10 K along both axes in the conducting plane. Note the clear change in shape from symmetric peaks to asymmetric peaks in the frequency range 250 to 300  $\text{cm}^{-1}$ .

Fanlike at higher frequencies. This behavior is characteristic of phase phonons as described by Rice.<sup>20</sup> These phonons are typically totally symmetric modes, which couple to the phase of the charge-density wave, with respect to the underlying lattice. The coupling of the phonons to the phase causes localized variations of the phase leading to a local electric dipole moment. Phase phonons can have unusually large spectral weight since they depend on the strength of the coupling. They also broaden significantly if they occur at frequencies above the optical gap edge since they are able to decay through the creation of electron hole pairs. This last property will be exploited to make an estimate of the optical gap position in our samples in the following section.

The phonons are similar to those seen in other materials such as  $\text{NbSe}_3$ .<sup>21</sup> The phase phonons in our data are seen both in the spectrum parallel to the CDW direction and perpendicular to this direction. The strength of some of the stronger modes can be determined by an approximate fitting to a Lorentzian with no background assumed for the  $c$ -axis fit and a linear background for the  $b$ -axis fit. This will only give a rough estimate of the phonon parameters since a full treatment requires fitting all phonons simultaneously as there is a significant degree of coupling between these phonons. Additionally, the assumption of no background conductivity for the  $c$  axis is likely incorrect. The intent here is to show the relative spectral strength in each mode. The positions  $\omega_0$ , linewidths  $\gamma$ , and oscillator strengths  $f$  of the phonons so treated for  $\eta$ - $\text{Mo}_4\text{O}_{11}$  are given in Table I. From Table I, we see that each linewidth is of the order of a few  $\text{cm}^{-1}$  and that the oscillator strengths are quite large (800–1200), which supports the assignment of these peaks as phase phonons rather than bare phonons.

This calculation was not extended to the phonons seen in  $\gamma$ - $\text{Mo}_4\text{O}_{11}$  due to the smaller size of the optical gap. Essentially all of the phonons seen in the  $\gamma$ - $\text{Mo}_4\text{O}_{11}$  spectra occur above the estimated optical gap and as a result will not ex-

TABLE I. The best-fit values of line width  $\Gamma_j$  and oscillator strength  $f_j$  of selected phonons at frequency  $\omega_j$  for  $\eta$ - $\text{Mo}_4\text{O}_{11}$  using a sum of Lorentzians to model  $\epsilon_1(\omega)$ ,  $\epsilon(\omega) = \epsilon_\infty + \omega_p^2 \sum_j f_j / (\omega_j^2 - \omega^2 - i\omega\Gamma_j)$ , where  $\epsilon_\infty = 0.8$ .

$\omega_j$ ( $\text{cm}^{-1}$ )	$\Gamma_j$ ( $\text{cm}^{-1}$ )	$f_j$
<i>c</i> axis		
197	3.1	1200
209	5.7	1731
<i>b</i> axis		
145.9	1.6	856
161.4	2.4	1286

hibit the strong spectral strength characteristic of the phonons within the optical gap region.

#### IV. DISCUSSION

In 1D CDW systems one expects a gap in the optical conductivity spectrum and a peak in the spectrum near the gap edge due to a discontinuity in the density of states in the CDW state. On the other hand, in a 2D system, a gap does not necessarily open symmetrically over the entire Fermi surface. In the high-temperature superconductors when the gap ( $T < T_c$ ), or pseudogap ( $T > T_c$ ), is not complete in all directions in  $k$  space, one does not see a clear gap feature in the optical conductivity.<sup>22,23</sup> This is because reflectance measurements are not selective in  $k$  space but instead average over the entire Brillouin zone. This will lead to the residual optical conductivity below the energy of the gap. With a large free-carrier population this can lead to a completely “filled-in” gap, so no gap would be seen optically.

Simply extrapolating the optical conductivity from our lowest measured frequency to zero frequency suggests a decreasing dc conductivity ( $\sigma_{dc}$ ) with lowering temperature, in disagreement with results of resistivity measurements.<sup>3</sup> In both Figs. 3 and 4, the dc conductivity is shown by a black square at low frequencies. If a square is not present, this indicates that the conductivity was higher than the upper bounds of the plot. The discrepancy between  $\sigma_{dc}$  and an extrapolation of the optical data is clear for the  $b$  and  $c$  axes  $\eta$ - $\text{Mo}_4\text{O}_{11}$  conductivity below 70 K.

We first consider the contribution from the remaining free carriers in the CDW state to the optical conductivity assuming a Drude functional form  $\sigma_1(\omega) = \omega_p^2 \tau / [4\pi(1 + \omega^2 \tau^2)]$ , which can be thought of as a Lorentzian peak centered at zero frequency. If this peak increases in height with decreasing temperature this would correspond to an increasing  $\sigma_{dc}$ . The half width of the Drude curve is determined by the scattering rate  $1/\tau$  of the free carriers that typically decreases with temperature as the phonon contribution is frozen out. The height of the curve is determined in part by the width and also by the number of remaining free carriers since  $\omega_p^2 = 4\pi n e^2 / m^*$ , where  $n$  is the carrier density. As free carriers are removed one expects the Drude peak height to decrease unless the width of the peak is also reduced.

There is some evidence of such a contribution in our spectra, particularly in the 85 K conductivity spectrum, where the gap starts to form  $\leq 400 \text{ cm}^{-1}$ , but below  $75 \text{ cm}^{-1}$  the conductivity increases again. At lower temperatures this increas-

ing conductivity disappears, perhaps corresponding to the Drude peak narrowing to below the measured frequency range. Dashed lines in Fig. 3 show the Drude contribution calculated for 85 K from published results. Note the fair agreement despite the fact that no attempt has been made to fit to this spectra. The Drude curves for lower temperatures are not shown because the widths are too narrow to be seen clearly on the plot. In fact a calculation of the width ( $\Gamma$ ) of a Drude from the carrier density determined by the Hall mobility<sup>8</sup> and using published resistivity measurements<sup>3</sup> gives a  $\Gamma \approx 50 \text{ cm}^{-1}$  at 85 K and significantly less ( $\leq 2 \text{ cm}^{-1}$ ) at 10 K. This calculation was made assuming no significant change in the effective mass of the free carriers; however, the mass would have to change by almost two orders of magnitude to result in any significant change to the spectral weight in our measurement region. Thus, in  $\eta\text{-Mo}_4\text{O}_{11}$  we can assume that the free-carrier component is well below our measured frequency range at the lowest temperatures and these spectra are relatively free from any effect of these free carriers.

While mechanisms other than a Drude peak do exist to give a nonzero dc conductivity—such as contributions from a low-frequency collective mode<sup>24</sup>—these mechanisms seem fundamentally inconsistent with the temperature dependence seen in the resistivity measurements. For instance, large frequency shifts in such a collective mode as a function of temperature would be required to cause the increasing  $\sigma_{dc}$  at the lower temperatures.

The plasma frequency for just the free-carrier component  $\omega_{pf}^2 = 4\pi n_f e^2 / m^*$  calculated for these model free-carrier Drude curves is  $\approx 300 \text{ cm}^{-1}$ . We expect a zero crossing of the frequency-dependent dielectric function  $\epsilon_1(\omega)$  at this frequency and indeed, for the  $c$ -axis dielectric spectra we see a zero crossing at  $\approx 58 \text{ cm}^{-1}$  in both  $\eta\text{-Mo}_4\text{O}_{11}$  and  $\gamma\text{-Mo}_4\text{O}_{11}$ . This lends support to the idea that the free-carrier contribution is well below our frequency range at 10 K.

On the other hand, in  $\gamma\text{-Mo}_4\text{O}_{11}$  with only one CDW transition, a significant proportion of free-carrier spectral weight remains even at 10 K. The dashed line in Fig. 4 shows the calculated Drude contribution for 10 K. Clearly, one has to be aware of this contribution when interpreting the measurements on this phase.

Secondly, we have estimated the plasma frequency  $\omega_p$  by integrating using a conductivity sum rule the spectral weight of the conductivity. This spectral weight is not just due to free carriers at temperatures below the transition temperature. While a rigorous calculation would require integrating from zero frequency to a frequency below interband excitations, we can see from our conductivity spectra that most of the spectral weight occurs below  $\approx 5000 \text{ cm}^{-1}$  and is not due to any interband transitions. Therefore, to a good approximation, we can integrate from our lowest frequency to  $5000 \text{ cm}^{-1}$ . Using this approximation gives a plasma frequency that is essentially temperature independent and has a value of  $\omega_p = 15\,500 \pm 1000 \text{ cm}^{-1}$  for  $\eta\text{-Mo}_4\text{O}_{11}$  along either the  $b$  or the  $c$  axes and for all temperatures. For  $\gamma\text{-Mo}_4\text{O}_{11}$ , the integration to  $5000 \text{ cm}^{-1}$  gives  $\omega_p = 13\,000 \pm 2000 \text{ cm}^{-1}$  for all temperatures. Both these values are in good agreement with the more definitive results from higher frequency measurements.<sup>17</sup>

In the  $\eta\text{-Mo}_4\text{O}_{11}$ , the fact that the direction perpendicular

to the CDW should most clearly show the optical gap is not completely unexpected. In the spin-density wave system,  $(\text{TMTSF})_2\text{PF}_6$ , Degiorgi *et al.*<sup>25</sup> could only clearly see the optical gap when measuring perpendicular to the spin-density wave direction but saw no clear evidence of a gap when parallel to this direction.

The edge of the optical energy gap cannot be clearly located but by  $250\text{--}300 \text{ cm}^{-1}$  the conductivity level can no longer be attributed solely to the phonon peaks. Following the procedure used by Katsufuji *et al.*<sup>26</sup> a linear extrapolation of the  $\sigma(\omega)$  at 10 K to the abscissa yields an estimate of the gap energy of  $\approx (215 \pm 35) \text{ cm}^{-1}$  from the  $c$ -axis spectra and  $\approx (165 \pm 40) \text{ cm}^{-1}$  from the  $b$ -axis spectra. Unfortunately, the presence of phonons in this region or broadening of the peak makes these linear extrapolations somewhat problematic. Transport measurements<sup>9</sup> place the gap edge at  $\approx 260 \text{ cm}^{-1}$  via fitting the dc resistivity, assuming thermally activated behavior.

The gap opening in the  $b$ -axis direction is not as complete. There is more conductivity than is seen in the  $c$ -axis spectra, in the region below  $225 \text{ cm}^{-1}$ , which seems to be related to the CDW itself. In Fig. 3, this spectral weight is indicated by the cross hatching. Although no definite determination has been made, the spectral weight in the gap could be due to some sort of broad midgap state. Such states have been seen in 1D incommensurate CDW materials<sup>27–29</sup> and are attributed to formation of boundaries between regions of different phases resulting in a soliton lattice structure. It has been suggested that this is a characteristic feature of an incommensurate CDW (Ref. 30). These midgap states are broad reststrahlenlike features and are not expected to be seen in spectra polarized perpendicular to the direction of the CDW.<sup>31</sup> We measured a second sample from a different batch and have confirmed that this feature is intrinsic to the material and not just to a particular crystal sample or growth batch.

The other predicted feature of a 1D CDW system, a peak at the edge of the gap, should be seen in the conductivity since it is a measure of the joint density of states above and below the Fermi level. While no sharp peak is seen here, there is a broad peak with a maximum in the range  $350\text{--}400 \text{ cm}^{-1}$ . Whether this peak is related to the gap is not clear due to the 2D nature of  $\text{Mo}_4\text{O}_{11}$ , however, the fact that it is seen in both polarizations is suggestive of it being related to the CDW.

In both polarizations some optical conductivity spectral weight appears to transfer from lower frequencies to the region of the  $400 \text{ cm}^{-1}$  peak as the temperature is lowered below the first CDW transition. This can be seen in Figs. 6(a) and 6(b) where  $\sigma_1(40 \text{ K})$ —at which temperature the CDW is almost fully formed—is divided by  $\sigma_1(115 \text{ K})$ , just above  $T_{C1}$ . These plots clearly demonstrate the transfer of spectral weight. In addition, it is reasonable to take the point that these ratios cross unity as an approximate upper estimate of the optical gap. If the CDW can still be regarded as a 1D phenomenon then this estimate should be accurate due to the expected peak at the gap edge in a 1D CDW system. Ignoring the sharp optical phonon peaks at lower frequencies, the crossing points for the  $b$  and  $c$  axes are in the range  $210\text{--}230 \text{ cm}^{-1}$  and  $260\text{--}280 \text{ cm}^{-1}$ , respectively, in good agreement with transport results. Figures 6(c) and 6(d) are similar plots

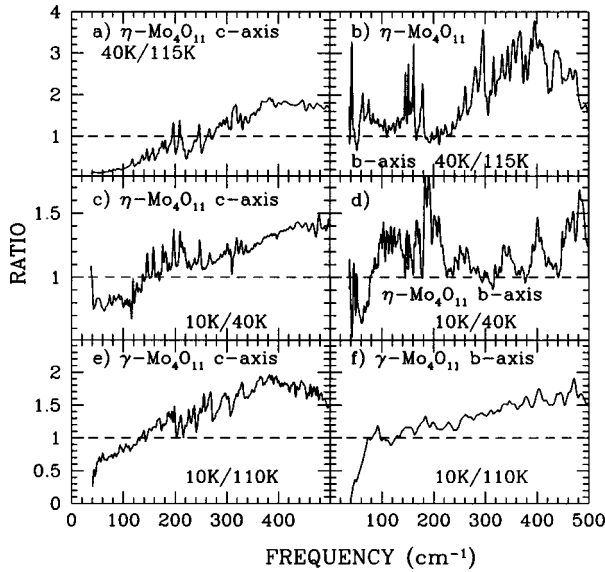


FIG. 6. Ratio of  $\sigma_1(\omega)$  well below the CDW transition by  $\sigma_1(\omega)$  just above the transition. This plot shows the transfer of the spectral weight that accompanies the formation of a CDW. The plots for  $\eta\text{-Mo}_4\text{O}_{11}$  are (a) and (b) for  $T_{C1} = 105$  K, (c) and (d) for  $T_{C2} = 35$  K, and the plots for  $\gamma\text{-Mo}_4\text{O}_{11}$  are for  $T_C = 100$  K. The crossing of unity can be considered as an upper estimate of the CDW optical gap.

for temperatures above (40 K) and below (10 K)  $T_{C2}$ . A similar, but smaller, transfer of spectral weight occurs with an estimated gap of  $\approx 140$   $\text{cm}^{-1}$  from the  $c$ -axis results and  $\approx 80$   $\text{cm}^{-1}$  from the  $b$ -axis plot. The CDW gap for the second transition, as determined by transport measurements,<sup>32</sup> is 73–78  $\text{cm}^{-1}$ .

Comparing Figs. 3 and 4, significant differences are seen between the conductivity of the  $\gamma$  and  $\eta$  phases. The reduction in the  $\gamma$ -phase conductivity at low frequencies is not as large as in  $\eta\text{-Mo}_4\text{O}_{11}$  and the rate of change with tempera-

ture is lower. This is in qualitative agreement with resistivity measurements.<sup>3</sup> In comparing the  $b$ -axis data to the  $c$ -axis data for  $\gamma\text{-Mo}_4\text{O}_{11}$ , it is interesting to note that the gap onset appears to occur at  $\approx 100$   $\text{cm}^{-1}$  in both polarizations. Figures 6(e) and 6(f) show the ratio of  $\sigma_1(10$  K) and  $\sigma_1(110$  K). The  $c$ -axis plot in Fig. 6(e) displays a transfer of spectral weight as seen with  $\eta\text{-Mo}_4\text{O}_{11}$  and gives an upper estimate of 125 to 145  $\text{cm}^{-1}$  for the gap edge and the  $b$ -axis plot in Fig. 6(f) has a unity crossing in the range 80 to 125  $\text{cm}^{-1}$ . Using a linear extrapolation of  $\sigma_1(10$  K) to the abscissa yields an estimate of the gap of  $(\approx 35 \pm 10)$   $\text{cm}^{-1}$  for both polarizations. Transport measurements<sup>9</sup> give a gap of  $\approx 105$   $\text{cm}^{-1}$  and angle-resolved photoemission spectroscopy (ARPES) measurements<sup>10</sup> give gaps ranging from 0 to 480  $\text{cm}^{-1}$ , depending on direction. Since optical measurements average over the Fermi surface one should expect to observe the smallest direct gap.

Table II shows a summary of the gap energy estimates from published transport measurements, and from our two methods of estimating the optical gap. As can be seen, the estimates derived from the ratios of conductivities are in agreement with the transport measurements while the estimates from the linear extrapolation to the abscissa are consistently lower. We attribute this discrepancy to the phonon peaks in the region, which make it difficult to derive a definitive linear fit to the slope. Additionally, due to the range of gap sizes one does not expect a sharp edge to appear at the gap energy.

The  $c$ -axis spectra of  $\gamma\text{-Mo}_4\text{O}_{11}$  show a very broad peak forming below the CDW transition but a similar structure is only weakly visible in the  $b$ -axis spectra. Since the electronic density from Hall measurements<sup>3</sup> for  $\gamma\text{-Mo}_4\text{O}_{11}$  is about 40 times what it is for  $\eta\text{-Mo}_4\text{O}_{11}$ , the weak peak in the  $b$ -axis data may be partially screened by the remaining free carriers. This remaining electronic density may also be responsible for masking some of the transfer of spectral weight along the  $b$  axis [see Fig. 6(f)].

TABLE II. Comparison of the CDW gap energies estimated from transport, ARPES, and optical measurements.

	$2\Delta_1$ ( $\text{cm}^{-1}$ )	$\eta\text{-Mo}_4\text{O}_{11}$ $2\Delta_2$ ( $\text{cm}^{-1}$ )	$\gamma\text{-Mo}_4\text{O}_{11}$ $2\Delta$ ( $\text{cm}^{-1}$ )
Transport	260	73,78	105
ARPES $2\Delta_{MAX}$		No data	$480 \pm 10$
Present work			
Linear extrapolation			
$b$ axis	130–205		25–45
$c$ axis	180–250		25–45
Present work			
Ratio			
$b$ axis	210–230	$\approx 80$	80–125
$c$ axis	260–280	$\approx 140$	125–145
Present work			
Phase phonons			
$b$ axis	250–300		
$c$ axis	250–300		$< 125$

As mentioned previously, if the phonon peaks are phase phonons it is possible to estimate the position of the gap edge from the change in the phonon shape as a function of frequency. Table II gives the estimates of the frequency range of the optical gap from the phonons. The estimates for  $\gamma$ - $\text{Mo}_4\text{O}_{11}$  are tentative since there are few phonons below the gap edge, which can be clearly seen. The upper range for this phase is based on the phonons becoming more asymmetric and less Lorentzian in profile. At frequencies significantly higher than the estimated gap edge ( $>1000\text{ cm}^{-1}$ ), our spectrum changes little with temperature and remains very much like the normal-state free-carrier spectra. Based on this observation, it is expected that most of the spectral changes seen in the FIR region are due to rearrangement of states near the Fermi energy.

One of the motivations for making these measurements was to compare 2D and 1D systems. The two-dimensional nature of these crystals complicates the simple picture of the one-dimensional Peierl's transition since it is not possible to nest an entire two-dimensional Fermi surface using a single wave vector. Canadell and co-workers have developed a theory, based on hidden one-dimensional Fermi surfaces,<sup>33-35</sup> which they have applied to  $\text{Mo}_4\text{O}_{11}$  and to a number of similar molybdenum bronzes. The Fermi surface is proposed to be made up of several one-dimensional Fermi surfaces with conduction occurring in bands with one-dimensional character. Angle-resolved photoemission spectra of a similar quasi-two-dimensional material  $\text{Na}_{0.9}\text{Mo}_6\text{O}_{17}$  lends some confirmation to the existence of such a Fermi surface.<sup>36,37</sup> However, Terrasi *et al.*<sup>10</sup> suggest that both one- and two-dimensional bands are involved in the gap opening.

One would expect the optical spectra of the "purple bronzes"<sup>18</sup> to be similar to that of  $\text{Mo}_4\text{O}_{11}$  due to the similarity of the structures of these materials. Both systems are made up of similar structural units, slabs of  $\text{MoO}_6$  octahedra with  $\text{MoO}_4$  tetrahedra joining them. Two of the investigated "purple bronzes"  $\text{Na}_{0.9}\text{Mo}_6\text{O}_{17}$  and  $\text{K}_{0.9}\text{Mo}_6\text{O}_{17}$  are two dimensional and the same atomic orbitals are expected to be involved in the conduction bands<sup>34</sup> as are in  $\text{Mo}_4\text{O}_{11}$ . These materials are known to have commensurate CDW's; the gap energies are the same order of magnitude as the  $\text{Mo}_4\text{O}_{11}$  crystals. One difference is that these materials are "doped" CDW materials while  $\text{Mo}_4\text{O}_{11}$  is a stoichiometric material. However, this difference aside, there are many similarities between the materials and both their band structures have been calculated in a similar procedure using the hidden 1D Fermi-surface hypothesis.<sup>34</sup>

While unfortunately no comparison can be made of the optical conductivity since this was not calculated for the "purple bronzes," the reflectance spectra of these materials bears a strong resemblance to that of  $\text{Mo}_4\text{O}_{11}$ . The spectra display a suppression of reflectance at low temperatures with an accompanying increase in a region above the depression. In the "purple bronzes" there appears to be a precursor of these features at room temperature, ascribed by Degiorgi *et al.*<sup>18</sup> to a "pseudogap," which is not evident in our spectra. No peaks corresponding to optically active phonons are observed in the reflectance spectra in contrast to those seen in the  $\text{Mo}_4\text{O}_{11}$  spectra.

Optical spectra of many other CDW materials have been measured, most are 1D and undergo a metal to insulator/

semiconductor transition. An exception  $\text{NbSe}_3$  has a metal-metal transition and its spectrum bears a strong resemblance to that of  $\eta$ - $\text{Mo}_4\text{O}_{11}$ .<sup>21</sup> The phase phonons and the increased conductivity at the gap edge are seen, as they are in our measurements. The low-frequency increase of conductivity in  $\text{NbSe}_3$  was attributed to the tail of the phason collective mode. In our measurements, we see no evidence of such tail at the lowest temperatures. Interestingly, a good theoretical description of some of the transport properties and the tunneling spectra of  $\text{NbSe}_3$  has been made using a quasi-two-dimensional model.<sup>38</sup>

Indeed, the optical spectra of  $\text{Mo}_4\text{O}_{11}$  shares many of the optical phenomena one sees in most of the different families of CDW materials from the 1D Bechgaard salts to the wide variety of forms of bronzes. The spectra of  $\text{K}_{0.3}\text{MoO}_3$  have been measured very completely and although this material is 1D and has a metal-insulator transition, it is a good model system of the optical spectra of a CDW material. As seen previously, our measurements display a peak at the gap edge, as is seen in  $\text{K}_{0.3}\text{MoO}_3$ , although the proximity of the phonon peaks obscures its structure and the gap-edge peak in  $\text{Mo}_4\text{O}_{11}$  is seen to have a similar shape as that of  $\text{K}_{0.3}\text{MoO}_3$ . Very strong phonon peaks are seen in both systems and in  $\text{K}_{0.3}\text{MoO}_3$  these are described as being phase phonons.<sup>39</sup> In  $\text{K}_{0.3}\text{MoO}_3$ , two strong sharp peaks are seen, the lower frequency peak was described as a phason mode and the other one is suggested to be related to a bound collective mode. In our spectra, no such modes are evident although it is possible that such modes exist below our spectral range. The spectra of  $\text{Rb}_{0.3}\text{MoO}_3$ ,<sup>31</sup> closely related to  $\text{K}_{0.3}\text{MoO}_3$ , show similar phase phonons and also includes a midgap peak as seen in our *b*-axis  $\eta$ - $\text{Mo}_4\text{O}_{11}$  spectra.

Taken as a whole, the spectra of  $\text{Mo}_4\text{O}_{11}$  are seen to exhibit virtually all the optical phenomena observed in 1D systems despite a reduced magnitude of spectral changes. This could be seen as an endorsement of the theory of Canadell and Whangbo, which implies that CDW transitions are inherently 1D in nature. However, one can note that materials such as chromium exhibit some of these same features, such as a conductivity suppression and a gap-edge peak, while being higher dimensional although the presence of a large free-carrier density obscures them.<sup>40,41</sup> Currently, there seems to be no complete theory that treats a material with the low degree of in-plane anisotropy (as is seen in  $\text{Mo}_4\text{O}_{11}$ ) and so no definite conclusions can be reached on this point.

In the area of high-temperature superconductivity, there has recently been great interest in "stripe" phases and their relationship to superconductivity in the cuprates. Recent optical work<sup>26</sup> on  $\text{La}_{1.67}\text{Sr}_{0.33}\text{NiO}_4$ , which is isostructural to the La superconductors, shows temperature-dependent structure similar to that which we have observed in  $\text{Mo}_4\text{O}_{11}$ . This material is a 2D doped Mott insulator that undergoes a charge-ordering phase transition driven by an electron-electron interaction. Although the gap magnitude ( $\approx 2100\text{ cm}^{-1}$ ) associated with the charge ordering is higher than is seen with  $\text{Mo}_4\text{O}_{11}$ , the change in the optical conductivity is very similar. Specifically, the low-frequency spectral weight is reduced, with a corresponding transfer of spectral weight to a broad peak above the edge of the energy gap. The larger gap energy allowed the authors to use the conductivity to directly estimate the optical gap, since the phonon structure

occurs well below the gap edge.

The charge ordering in  $\text{La}_{1.67}\text{Sr}_{0.33}\text{NiO}_4$  is accompanied by a corresponding spin-ordering;<sup>26</sup> optically, these two types of ordering will exhibit similar spectra. The carriers order in “stripes” and act as domain walls for antiferromagnetic domains making this system more complex than  $\text{Mo}_4\text{O}_{11}$  despite the qualitatively similar optical spectra. In both  $\text{Mo}_4\text{O}_{11}$  (Guyot *et al.*<sup>42</sup>) and  $\text{La}_{1.67}\text{Sr}_{0.33}\text{NiO}_4$  (Vigliante *et al.*<sup>43</sup>) the x-ray peak, which appears due to the lattice rearrangement at the CDW transition, is very weak suggesting that both systems have weak coupling driving the transition.

Of wider significance is the observation that the same form of charge ordering has been observed<sup>44</sup> in  $\text{La}_{1.6-x}\text{Nd}_{0.4}\text{Sr}_x\text{CuO}_4$  in coexistence with superconductivity, although optical measurements<sup>45</sup> do not show the same strong rearrangement of spectral weight seen in our measurements. The “stripe” phase with its spin/charge-density wave formation has been suggested as a possible cause of the “pseudogap” seen in underdoped high-temperature superconductors<sup>46–48</sup> in the normal state and as the source of high-temperature superconductivity via the spatial restriction of the metallic stripes. Understanding the spatial ordering of spin and charge in these materials is important since it is believed that it may be interactions with the spins that mediates the superconductivity, rather than the traditional electron-phonon interaction.

## V. CONCLUSIONS

We have performed FIR optical measurements of the *b-c* conducting plane in both phases of the charge-density wave material  $\text{Mo}_4\text{O}_{11}$ . We have found in measuring the CDW phase of  $\text{Mo}_4\text{O}_{11}$  that the 2D system does seem to have features characteristic of a 1D system. Evidence of an optical gap is clearly seen in the optical conductivity despite the gap being zero in certain directions of *k* space. The optical-gap values estimated from the spectra are in agreement with the

results of transport measurements. A broad peak appears in the spectrum centered in the range of the edge of the gap as determined by transport measurements. This peak is believed to be the peak typically seen at the edge of a CDW gap although it is not clear that such a feature should occur in a 2D system; this aspect is being pursued further. No evidence is seen of a collective mode in these materials, although some sort of midgap state is seen in measurements polarized parallel to the CDW direction.

Many phonons closely resembling the phase phonons described by Rice<sup>20</sup> are seen in the spectra below the CDW transition both parallel and perpendicular to the CDW direction. A complete analysis of the phonons along with an assignment of modes requires measurement of the *a*-axis excitation spectrum and comparison to other techniques such as Raman measurements. Such an analysis is underway and will be published separately.

Although certainly a different physical system from the high-temperature superconductors,  $\text{Mo}_4\text{O}_{11}$  potentially provides a model system of the spectral response of a 2D CDW system; the similarity of transition temperatures and energy gaps aid in this comparison. For instance, measurement of  $\text{Mo}_4\text{O}_{11}$  allows one to investigate the effect the CDW formation has on conduction in a 2D plane and if one expects anisotropy in the plane to be seen optically.

## ACKNOWLEDGMENTS

This work was supported by the National Science and Engineering Research Council (NSERC), and Simon Fraser University, and the U.S. Department of Energy, Division of Materials Science, Contract No. DE-AC02-98CH10886. A.W.M. gratefully acknowledges Dr. J. Musfeldt, Zhengtao Zhu, and co-workers for use of their high-frequency measurements and for many extremely useful discussions on the results.

- 
- <sup>1</sup>H. Guyot, C. Escribe-Filippini, G. Fourcaudot, K. Konate, and C. Schlenker, *J. Phys. C* **16**, L1227 (1983).  
<sup>2</sup>P. Foury and J. P. Pouget, *Int. J. Mod. Phys. B* **7**, 3973 (1993).  
<sup>3</sup>M. Inoue, S. Ohara, S. Horisaka, M. Koyano, and H. Negishi, *Phys. Status Solidi B* **148**, 659 (1988).  
<sup>4</sup>S. Ohara, M. Koyano, H. Negishi, M. Sasaki, and M. Inoue, *Phys. Status Solidi B* **164**, 243 (1991).  
<sup>5</sup>S. Ohara, H. Negishi, and M. Inoue, *Phys. Status Solidi B* **172**, 419 (1992).  
<sup>6</sup>M. Sasaki, Y. Hara, M. Inoue, T. Takamasu, N. Miura, G. Machel, and M. von Ortenberg, *Phys. Rev. B* **55**, 4983 (1997).  
<sup>7</sup>M. Ghedira, H. Vincent, M. Marezio, J. Marcus, and G. Fourcaudot, *J. Solid State Chem.* **56**, 66 (1985).  
<sup>8</sup>M. Sasaki, G. X. Tai, S. Tamura, and M. Inoue, *Phys. Rev. B* **47**, 6216 (1993).  
<sup>9</sup>W. Gao, M. Sasaki, H. Negishi, M. Inoue, and V. A. Kulbachinskii, *J. Phys. Soc. Jpn.* **64**, 518 (1995).  
<sup>10</sup>A. Terrasi, M. Marsi, H. Berger, F. Gauthier, L. Forro, G. Margaritondo, R. J. Kelley, and M. Onellion, *Z. Phys. B* **100**, 493 (1996).  
<sup>11</sup>G. Travaglini, P. Wachter, J. Marcus, and C. Schlenker, *Solid State Commun.* **37**, 599 (1981).  
<sup>12</sup>L. Degiorgi, B. Alavi, G. Mihály, and G. Grüner, *Phys. Rev. B* **44**, 7808 (1991).  
<sup>13</sup>H. Guyot, E. Al Khoury, J. Marcus, C. Schlenker, M. Banville, and S. Jandl, *Solid State Commun.* **79**, 307 (1991).  
<sup>14</sup>H. Gruber, E. Krautz, H. P. Fritzer, K. Gatterer, and A. Popitsch, *Phys. Status Solidi A* **86**, 749 (1984).  
<sup>15</sup>M. Shimoda, K. Yagisawa, M. Okochi, and A. Yoshikawa, *J. Mater. Sci. Lett.* **6**, 1331 (1987).  
<sup>16</sup>M. Okochi, M. Shimada, and K. Yagisawa, *J. Mater. Sci. Lett.* **7**, 599 (1988).  
<sup>17</sup>Z. Zhu, J. Musfeldt, J. Sarrao, and Z. Fisk (unpublished).  
<sup>18</sup>L. Degiorgi, P. Wachter, M. Greenblatt, W. H. McCarroll, K. V. Ramanujachary, J. Marcus, and C. Schlenker, *Phys. Rev. B* **38**, 5821 (1988).  
<sup>19</sup>C. C. Homes, M. Reedyk, D. C. Crandles, and T. Timusk, *Appl. Opt.* **32**, 2976 (1993).  
<sup>20</sup>M. Rice, *Phys. Rev. Lett.* **37**, 36 (1976).  
<sup>21</sup>W. A. Challenor and P. L. Richards, *Solid State Commun.* **52**, 117 (1984).

- <sup>22</sup>T. Timusk and D. Tanner, in *Physical Properties of High Temperature Superconductors I*, edited by D. Ginsberg (World Scientific, Singapore, 1989), p. 339.
- <sup>23</sup>S. Tajima, *Supercond. Rev.* **2**, 125 (1997).
- <sup>24</sup>G. Travaglini and P. Wachter, *Phys. Rev. B* **30**, 1971 (1984).
- <sup>25</sup>L. Degiorgi, M. Dressel, Z. Schwartz, B. Alavi, and G. Grüner, *Phys. Rev. Lett.* **76**, 3838 (1996).
- <sup>26</sup>T. Katsufuji, T. Tanabe, T. Ishikawa, Y. Fukuda, T. Arima, and Y. Tokura, *Phys. Rev. B* **54**, 14 230 (1996).
- <sup>27</sup>M. Lind and J. Stanford, *Phys. Lett.* **39A**, 5 (1972).
- <sup>28</sup>K. Machida and M. Fujita, *Phys. Rev. B* **30**, 5284 (1984).
- <sup>29</sup>M. Itkis and F. Y. Nad', *Pis'ma Zh. Eksp. Teor. Fiz.* **39**, 373 (1984) [*JETP Lett.* **39**, 449 (1984)].
- <sup>30</sup>K. Machida and M. Nakano, *Phys. Rev. Lett.* **55**, 1927 (1985).
- <sup>31</sup>S. Jandl, M. Banville, C. Pépin, J. Marcus, and C. Schlenker, *Phys. Rev. B* **40**, 12 487 (1989).
- <sup>32</sup>M. Inoue, G. Machel, I. Laue, M. von Ortenberg, and M. Sasaki, *Phys. Status Solidi B* **172**, 431 (1992).
- <sup>33</sup>E. Canadell, M.-H. Whangbo, C. Schlenker, and C. Escribano-Filippini, *Inorg. Chem.* **28**, 1466 (1989).
- <sup>34</sup>E. Canadell and M.-H. Whangbo, *Chem. Rev.* **91**, 965 (1991).
- <sup>35</sup>E. Canadell and M.-H. Whangbo, *Int. J. Mod. Phys. B* **7**, 4005 (1993).
- <sup>36</sup>K. Breuer, C. Stagerescu, K. E. Smith, M. Greenblatt, and K. Ramanujachary, *Phys. Rev. Lett.* **76**, 3172 (1996).
- <sup>37</sup>G. H. Gweon, J. W. Allen, J. A. Clack, Y. X. Zhang, A. D. M Poirier, P. J. Benning, C. G. Olson, J. Marcus, and C. Schlenker, *Phys. Rev. B* **55**, 13 353 (1997).
- <sup>38</sup>X.-Z. Huang and K. Maki, *Phys. Rev. B* **40**, 2575 (1989).
- <sup>39</sup>L. Degiorgi and G. Grüner, *Synth. Met.* **55-57**, 2688 (1993).
- <sup>40</sup>A. S. Barker, B. I. Halperin, and T. M. Rice, *Phys. Rev. Lett.* **20**, 384 (1968).
- <sup>41</sup>A. S. Barker and J. A. Ditzenberger, *Phys. Rev. B* **1**, 4378 (1970).
- <sup>42</sup>H. Guyot, C. Schlenker, G. Fourcaudot, and K. Konaté, *Solid State Commun.* **54**, 909 (1985).
- <sup>43</sup>A. Vigliante, M. von Zimmermann, J. R. Schneider, T. Frello, N. H. Andersen, J. Madsen, D. J. Buttrey, D. Gibbs, and J. M. Tranquada, *Phys. Rev. B* **56**, 8248 (1997).
- <sup>44</sup>J. Tranquada, J. D. Axe, N. Ichikawa, A. R. Moodenbaugh, Y. Nakamura, and S. Uchida, *Phys. Rev. Lett.* **78**, 338 (1997).
- <sup>45</sup>S. Tajima, N. L. Wang, M. Takaba, N. Ichikawa, and S. Uchida, *J. Phys. Chem. Solids* (to be published).
- <sup>46</sup>I. Eremin, M. Eremin, S. Varlamov, D. Brinkmann, M. Mali, and J. Roos, *Phys. Rev. B* **56**, 11 305 (1997).
- <sup>47</sup>T. Dahm, D. Manske, and L. Tewordt, *Phys. Rev. B* **56**, R11 419 (1997).
- <sup>48</sup>V. J. Emery, S. A. Kivelson, and O. Zachar, *Phys. Rev. B* **56**, 6120 (1997).